The EMBO Journal vol.15 no.5 pp.955–963, 1996

Cystic fibrosis mice carrying the missense mutation G551D replicate human genotype–phenotype correlations

Stephen J.Delaney[1], Eric W.F.W.Alton[2], Stephen N.Smith[2], Dominic P.Lunn[1], Ray Farley[2], Paul K.Lovelock[1], Scott A.Thomson[1], David A.Hume[1], David Lamb[4], David J.Porteous[3], Julia R.Dorin[3] and Brandon J.Wainwright[1,5]

[1]Centre for Molecular and Cellular Biology, University of Queensland, Brisbane, 4072 Australia, [2]Ion Transport Unit, National Heart and Lung Institute, Manresa Road, London SW3 6LR, [3]MRC Human Genetics Unit, Western General Hospital, Crewe Road, Edinburgh EH4 2XU and [4]Department of Pathology, The University of Edinburgh, Medical School, Teviot Place, Edinburgh EH8 9AG, UK

[5]Corresponding author

We have generated a mouse carrying the human G551D mutation in the cystic fibrosis transmembrane conductance regulator gene (*CFTR*) by a one-step gene targeting procedure. These mutant mice show cystic fibrosis pathology but have a reduced risk of fatal intestinal blockage compared with 'null' mutants, in keeping with the reduced incidence of meconium ileus in G551D patients. The G551D mutant mice show greatly reduced CFTR-related chloride transport, displaying activity intermediate between that of *cftr*^{m1UNC} replacement ('null') and *cftr*^{m1HGU} insertional (residual activity) mutants and equivalent to ~4% of wild-type CFTR activity. The long-term survival of these animals should provide an excellent model with which to study cystic fibrosis, and they illustrate the value of mouse models carrying relevant mutations for examining genotype–phenotype correlations.

Keywords: animal models/cystic fibrosis/gene targeting/genotype–phenotype correlations/meconium ileus

Introduction

An important goal in the field of human genetics is to understand the relationship between gene function and disease pathophysiology. Cystic fibrosis (CF) is the most common lethal genetic disorder in the Caucasian population, and is caused by mutations in the cystic fibrosis transmembrane conductance regulator (CFTR). We, and others, have produced mouse models for CF in which mutations have been introduced into the murine *CFTR* gene (*Cftr*) by homologous recombination in embryonal stem (ES) cells (reviewed in Dorin *et al.*, 1994a). These animals demonstrate both the characteristic CF chloride defect and intestinal pathology typical of this disease. They have also proved useful in pre-clinical studies of *CFTR* gene transfer using correction of the chloride transport deficit as the primary measure of efficacy (Alton *et al.*, 1993; Hyde *et al.*, 1993; Grubb *et al.*, 1994). However, the available models carry grossly disrupted alleles, resulting either in no CFTR protein, exemplified by the 'null' *cftr*^{m1UNC} gene replacement event (Snouwaert *et al.*, 1992), or very low levels of normal protein, as in the case of the *cftr*^{m1HGU} gene insertion event (Dorin *et al.*, 1994b). In contrast, the majority of CF patients carry subtle mutations which result in the production of a dysfunctional mutant protein (Tsui, 1992). The effect of ectopic expression of normal CFTR on a mutant *CFTR* background is unknown and it may, therefore, be important and instructive to carry out such gene transfer studies in a mouse engineered to carry a mutant form of CFTR equivalent to that which occurs in CF subjects.

G551D is one of the most ancient and common CF mutations, with a world-wide frequency averaging 3% but found at higher frequencies in populations of Celtic descent (Hamosh *et al.*, 1992). In humans, G551D CFTR protein is processed normally but produces cAMP-regulated chloride channels showing markedly reduced function (Class III mutation) (Welsh and Smith, 1993). A key aspect of this mutation is the 3-fold reduction in the incidence of meconium ileus (neonatal intestinal blockage) in CF patients carrying the G551D mutation compared with patients homozygous for the most common *CFTR* mutation, ΔF508 (Hamosh *et al.*, 1992). We have used a single-step targeting strategy to introduce the human missense mutation G551D into mice, allowing us to determine whether this protective effect is substantiated across species and allowing for the first time the examination of CF genotype–phenotype correlations in the laboratory.

We have examined the histological features and determined the electrophysiological responses of the G551D mutant mice, and show that the phenotype is intermediate between that of existing *cftr*^{m1UNC} replacement ('null') and *cftr*^{m1HGU} insertional (residual activity) mutant mice. Importantly, intestinal blockage is reduced and survival increased in comparison with the 'null' *cftr*^{m1UNC} mutant mouse, mimicking the mild intestinal phenotype of G551D patients. In man, only a small number of CF phenotype–genotype correlations have been established (Hamosh and Cutting, 1993). This study indicates, therefore, how mice carrying relevant mutations may be used to test phenotype–genotype correlations which are difficult to establish clinically. These may be difficult to establish either because the numbers of patients with particular mutations are low or because any intrinsic effects are submerged by environmental or epigenetic factors.

Results

Generation of G551D mice

R1 ES cells were electroporated with the linearized targeting construct (Figure 1A) which carries both the G551D mutation and neomycin-selectable marker sequences. To minimize disruption of the transcription of the targeted

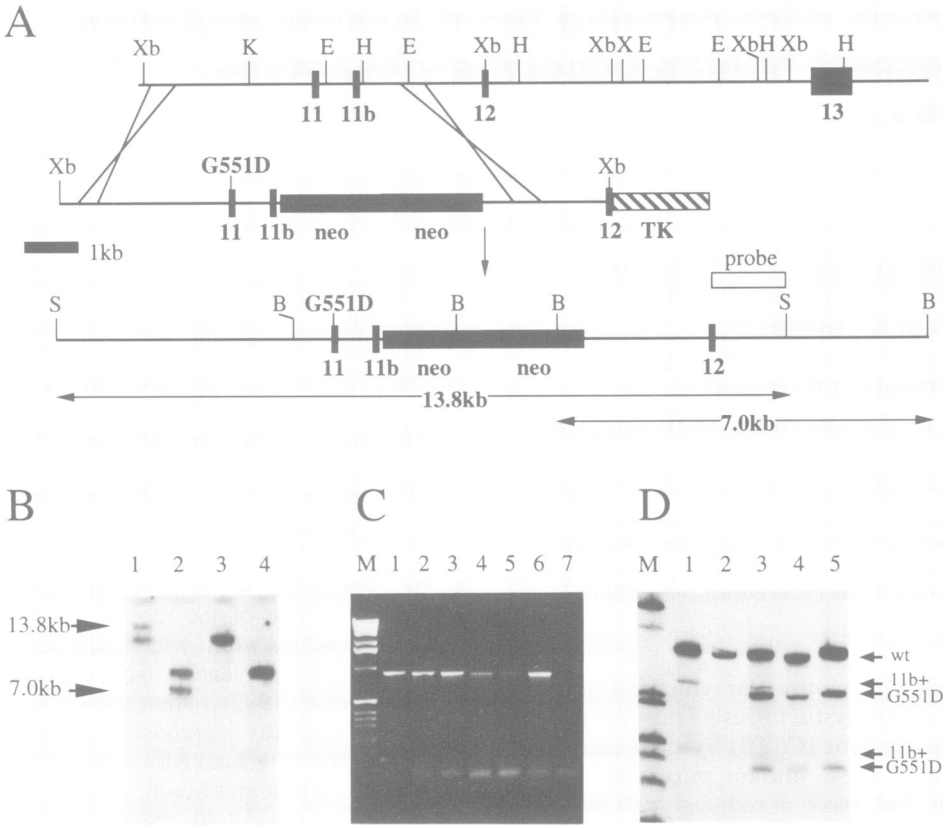

Fig. 1. Generation of mice carrying the G551D mutation. (**A**) Targeting of exon 11 to produce the G551D mutation; the genomic region of the *Cftr* gene cloned is shown at the top, exons 11, 11b, 12 and 13 are represented by filled boxes; *Eco*RI (E), *Hin*dIII (H), *Kpn*I (K), *Xho*I (X) and *Xba*I (Xb) restriction enzyme sites are indicated. The targeting construct shown below contains a 6.3 kb *Xba*I genomic fragment into which two *pgk–neo* expression cassettes have been inserted, both in the same orientation as that of the *Cftr* gene. A HSV-TK expression cassette (hatched box) is situated at the 3′ end, together with vector sequences (not shown). The structure of the genomic locus following targeting is shown at the bottom. The sizes of novel *Sac*I, S and *Bst*XI, B, restriction enzyme fragments identified by an external 3′ probe are indicated. (**B**) Representative Southern blot performed on ES cell DNA with the probe indicated in (A); targeted colony (lanes 1 and 2), non-targeted colony (lanes 3 and 4) digested with *Sac*I (lanes 1 and 3) and *Bst*XI (lanes 2 and 4). The sizes of the novel restriction enzyme fragments generated by the targeting event are indicated at the left of the panel. (**C**) The absence of novel splice variants in G551D animals is shown by RT-PCR performed on RNA prepared from wild-type (lane 1), $+/cftr^{G551D}$ (lane 2) and $cftr^{G551D}/cftr^{G551D}$ mice (lanes 3–6). Lanes 1–3, small intestine; lane 4, kidney; lane 5, lung; lane 6, testis; lane 7, no RNA control. (**D**) Quantitation of G551D transcripts by RT-PCR. To distinguish wild-type and G551D transcripts, all products have been digested with *Bsa*I. Lanes 1 and 2 are reactions performed on tissues from a wild-type mouse, lanes 3–5 are reactions carried out on RNA from a $+/cftr^{G551D}$ animal. Lanes 1 and 3, testis RNA; lanes 2 and 4, kidney RNA; lane 5, small intestine RNA. The identity of the bands detected is shown at the right of the panel.

allele, selectable marker sequences were positioned adjacent to exon 11b which is skipped in somatic CFTR transcripts (Delaney *et al.*, 1993). Targeting of the *Cftr* locus in ES cells by homologous recombination was identified by Southern blot analysis (Figure 1B). This occurred in 37 of 96 ES colonies obtained under positive/negative selection. Fifteen of 18 targeted colonies tested by allele-specific PCR retained the G551D allele. Five of these lines were used to generate chimaeric animals, and two males from independent cell lines showed germ-line transmission. Approximately half of the progeny of the two transmitting males were heterozygous for the G551D allele, as determined by allele-specific PCR (data not shown). We have designated this allele $cftr^{TgHm1G551D}$ but will refer to it in this manuscript as $cftr^{G551D}$. These heterozygous animals were inter-crossed to produce wild-type (+/+), heterozygous ($+/cftr^{G551D}$) and homozygous mutant ($cftr^{G551D}/cftr^{G551D}$) offspring. In agreement with the expected ratio of 1:2:1, in 123 animals genotyped from these crosses, 23% were +/+, 48% were $+/cftr^{G551D}$ and 29% were $cftr^{G551D}/cftr^{G551D}$. RT-PCR carried out on RNA prepared from a variety of tissues from heterozygous and homozygous animals indicated that selectable marker sequences retained in the targeted allele were not being incorporated as novel additional exons into CFTR transcripts (Figure 1C). Semi-quantitative RT-PCR indicated that the level of transcription of the G551D allele in a variety of tissues was ~53% of that of the wild-type allele (Figure 1D).

Intestinal obstruction is responsible for perinatal lethality and is reduced in G551D mutant mice compared with $cftr^{m1UNC}$ ('null') mice

In crosses between heterozygous animals, $cftr^{G551D}/cftr^{G551D}$ offspring were runted and between 50 and 70% of the weight of normal siblings. In matings maintained in specific pathogen-free conditions, ~33% of homozygous animals (46/141) died from intestinal obstruction before 35 days after birth (Figure 2). The site of intestinal obstruction in most animals, regardless of age, was just

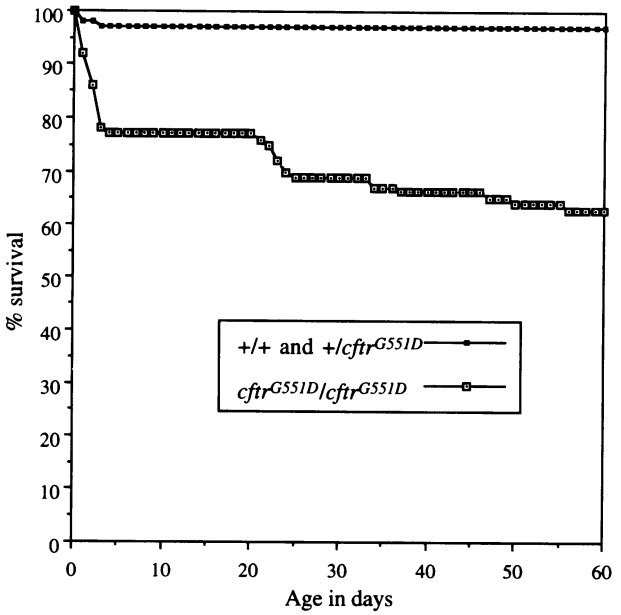

Fig. 2. Viability of $cftr^{G551D}/cftr^{G551D}$ animals. The survival of animals reared in specific pathogen-free conditions is shown. $cftr^{G551D}/cftr^{G551D}$ n = 141, +/+ and $+/cftr^{G551D}$ n = 67.

distal or proximal to the caecum, and the cause of death appeared to be peritonitis due to intestinal perforation.

To compare directly the relative survival of mice carrying different *Cftr* mutant alleles, animals were reared and housed in the same facility. The survival at 35 days was 8% (2/27) for the $cftr^{m1UNC}$ animals and 27% (12/44) for the $cftr^{G551D}$ animals. Survival of $cftr^{m1HGU}$ mutants was 93% as previously determined (Dorin *et al.*, 1994b). The reason for the reduction in survival of G551D mice in the common facility is uncertain, but most likely reflects the transfer from a specific pathogen-free to a standard animal facility and a concomitant change of food and bedding. The survival of the G551D mice was nevertheless significantly higher than for $cftr^{m1UNC}$ mutants ($P<0.05$).

Histopathological abnormalities in G551D animals

Histological examination of the intestinal tract of 15 $cftr^{G551D}/cftr^{G551D}$ adult animals of various ages revealed abnormalities in all mutant mice when compared with control ($+/cftr^{G551D}$ or +/+) siblings, regardless of intestinal obstruction. The small intestines of mutant animals showing obstruction were grossly abnormal, with loss of the villi and the accumulation of necrotic and faecal material in the lumen (Figure 3B). The most characteristic abnormality found in all of the apparently healthy mutant mice examined was the presence of eosinophilic concretions in the crypts of Lieberkühn. This results in the dilation of some crypts, particularly in the jejunum (Figure 3C and D). The colon of some animals also showed dilated mucus glands (data not shown).

In keeping with previous studies of the $cftr^{m1UNC}$ (Snouwaert *et al.*, 1992) and $cftr^{m1HGU}$ mutant mice (Dorin *et al.*, 1992), no difference in the appearance of the acinar or epithelial cells of the pancreas was detected between $cftr^{G551D}/cftr^{G551D}$ animals and control siblings. The lungs of 10 animals were also examined histologically and scored for cellularity of the lung parenchyma, expansion of the lung, crenation of the airway epithelia and epithelial hyperplasia. Using these criteria, no difference could be detected between homozygous animals and control siblings. No abnormalities were detected in the epithelia of the trachea or pharynx of nine $cftr^{G551D}/cftr^{G551D}$ animals, but three showed inspissated eosinophilic material in the lumen of the pharyngeal submucosal glands (Figure 4A and B).

In three of seven mutant animals suffering from intestinal obstruction, the gallbladder appeared black and enlarged. Abnormalities were also evident in a number of healthy mutant animals, and included gallbladders which were black, enlarged or reduced in size. Five of nine gallbladders from $cftr^{G551D}/cftr^{G551D}$ animals showed the presence of large numbers of polymorphonuclear cells, particularly eosinophils, in the gallbladder wall. In two of these animals, the gallbladder wall had an extremely vacuolated appearance in addition to the presence of inflammatory cells (Figure 4C and D). Abnormalities were also evident in the biliary tree of the liver. In three of 15 animals there was hyperplasia of the bile duct epithelia and in one of these animals there were bile pigments in the hepatocytes. Another of these three apparently healthy mutant animals showed focal biliary cirrhosis. In the area of focal cirrhosis, the biliary ducts were completely absent and were replaced by a fibrotic stroma and an inflammatory infiltrate characterized by large numbers of eosinophils (Figure 4E and F). Elsewhere in the liver, other than some bile ducts showing hyperplasia, the tissue was unremarkable.

Salivary gland defects have been reported in CF individuals and other CF mouse models (Ratcliff *et al.*, 1993). In two out of 10 G551D animals examined, the gland appeared hypercellular due to the serous cells having lost their vacuolated appearance (Figure 4G and H). The reproductive tract of five female and four male G551D animals appeared normal in comparison with control animals.

Electrophysiological responses of the $cftr^{G551D}/cftr^{G551D}$ mice

In comparison with wild-type litter mates, sodium-related measurements [baseline potential difference (PD) and response to amiloride] were significantly ($P<0.001$) increased in the nasal epithelium of $cftr^{G551D}/cftr^{G551D}$ mice *in vivo* (Figure 5A and B). The baseline PD profile closely resembles that seen in man, with a gradual increase in PD within the nasal cavity. Furthermore, the maximal value was reached at a greater distance from the external nares in the mutant mice, similar to the case in CF subjects. Subsequent perfusion with the cAMP-related agonist forskolin produced no response in the mutant mice; typically a depolarization was seen (Figure 5C). Finally, perfusion with ATP produced no significant difference between the calcium-related chloride secretion of the two genotypes (Figure 5D). In the trachea, *in vitro* measurements of baseline short circuit current (I_{SC}) or response to amiloride showed no significant difference between genotypes (Figure 5 legend), although the G551D mutant mice tended to have reduced values for both responses. Subsequent addition of forskolin produced a significantly ($P<0.01$) reduced response in the mutant

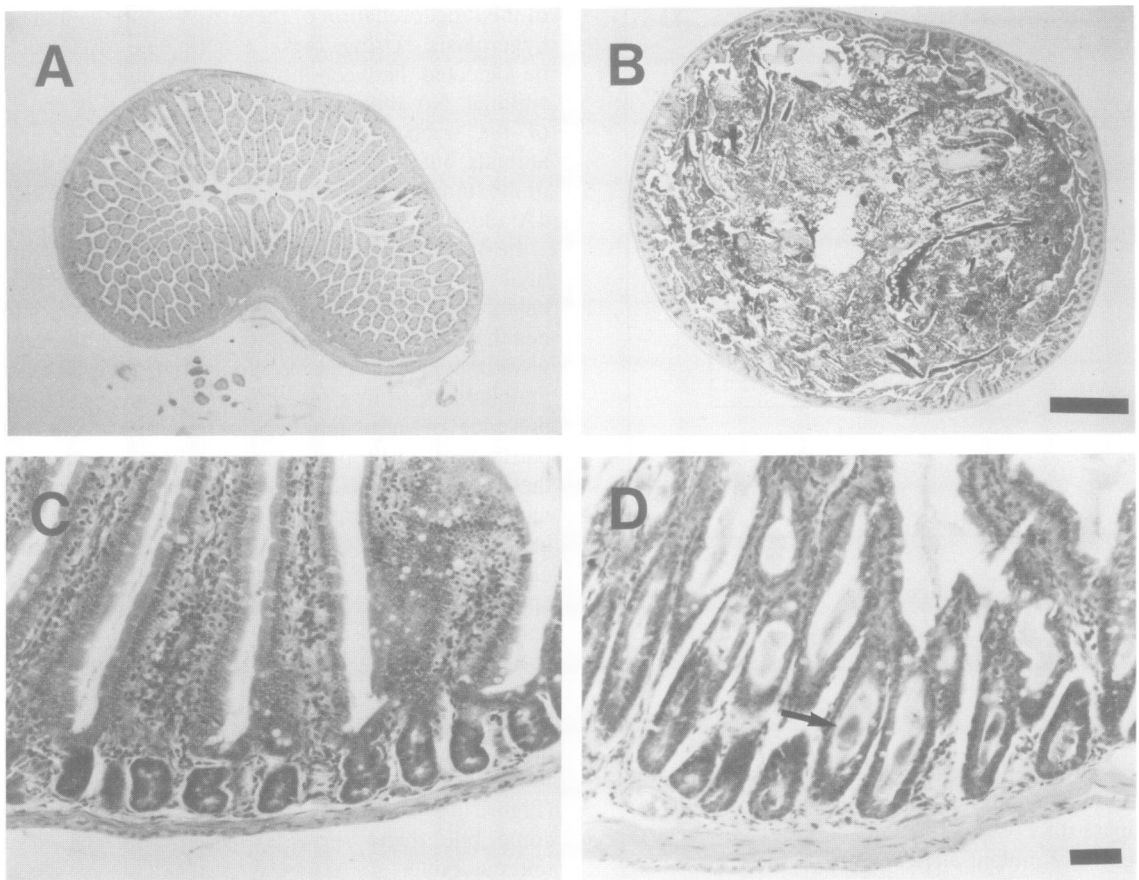

Fig. 3. Gut pathology of $cftr^{G551D}/cftr^{G551D}$ animals. (**A**) and (**C**) are tissues dissected from +/+ or $+/cftr^{G551D}$ animals; (**B**) and (**D**) are from G551D homozygotes. (A) and (B) are stained with PAS; (C) and (D) are stained with haemotoxylin and eosin. (A) and (B) are transverse sections of the small intestine. (C) and (D) are transverse sections of the wall of the jejunum; in the $cftr^{G551D}/cftr^{G551D}$ animal (D), apparently healthy when sacrificed, eosinophilic concretions are present in the crypts of Lieberkühn (arrowed). For each tissue, control and $cftr^{G551D}/cftr^{G551D}$ samples are shown at the same magnification. Scale bar: (A) and (B), 450 μm; (C) and (D), 50 μm.

mice (Figure 5E), whilst ATP responses were significantly ($P<0.05$) greater in the mutant mice (Figure 5E legend).

Throughout the intestinal tract, whether studied *in vitro* (jejunum and caecum) or *in vivo* (rectum), both baseline values and the response to forskolin were significantly ($P<0.001$) reduced (Figure 6). We, and others, have demonstrated previously that the response of wild-type mice to forskolin principally relates to chloride secretion (Alton *et al.*, 1993). This was confirmed in the present study by the subsequent addition of bumetanide (Figure 6). We also attempted to assess the effect of ionomycin (5 μM) added at the peak of the forskolin response. In both genotypes, this addition produced variable small changes, in keeping with CFTR acting as the principal chloride channel in the intestinal tract. Thus, in all tissues studied, the animals are characterized by a marked reduction in CFTR-related bioelectric responses.

The most frequent site of intestinal obstruction for $cftr^{G551D}/cftr^{G551D}$ animals was near the caecum, and the apparent protection against intestinal obstruction relative to $cftr^{m1UNC}/cftr^{m1UNC}$ 'null' mutant mice might result from residual CFTR-related chloride conductance in this region. For comparison, we therefore also measured *in vitro* forskolin responses in $cftr^{m1UNC}/cftr^{m1UNC}$ mice. In these animals, forskolin responses in the caecum were small, variable and frequently depolarizing, equivalent in magnitude to ~0.5% (0.8) of wild-type values. In contrast, $cftr^{G551D}/cftr^{G551D}$ animals show a residual caecal forskolin response (Figure 6B) significantly ($P<0.05$) greater than those of $cftr^{m1UNC}/cftr^{m1UNC}$ mice equivalent to ~4.9% (1.3) of wild-type values. In the jejunum, forskolin responses in $cftr^{G551D}/cftr^{G551D}$ mice also tended to be greater than those in $cftr^{m1UNC}/cftr^{m1UNC}$ mice equivalent to ~2.9% (3.3) of wild-type values.

Discussion

We have used a single-step gene targeting procedure to produce mice carrying the equivalent of the common human mutation G551D by placing the marker sequences necessary to select for homologous recombination events adjacent to an exon which is skipped in somatic cells. In common with existing CFTR 'null' mouse mutants, G551D mutant mice display runting, intestinal obstruction, gallbladder abnormalities and alterations in serous and mucous glands, and show an absence of frank pathology in the lungs, pancreas and reproductive tract. The pathological changes seen in the liver and biliary tract are similar to the focal biliary cirrhosis seen in 5% of CF patients (Park and Grand, 1991) and are of specific interest as they have not been reported previously in other CF mouse models. This may reflect the combined effect of

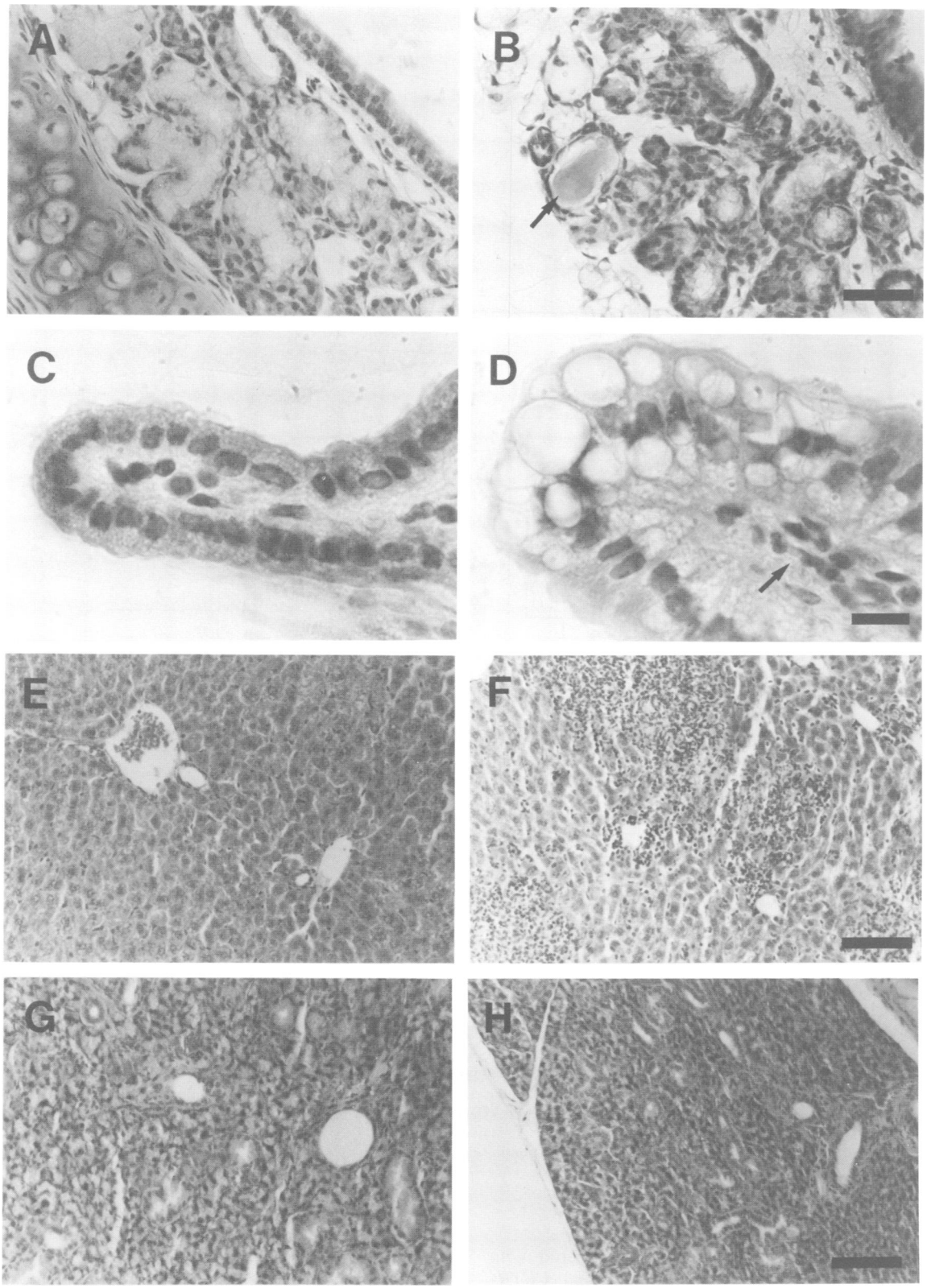

Fig. 4. Pathology of G551D animals in epithelial lined tissues. (**A**), (**C**), (**E**) and (**G**) are tissues from +/+ or +/$cftr^{G551D}$ animals; (**B**), (**D**), (**F**) and (**H**) from $cftr^{G551D}/cftr^{G551D}$ animals. All animals were apparently healthy when sacrificed. (A) and (B) Mucosal glands from behind the pharynx. The $cftr^{G551D}/cftr^{G551D}$ animal (B) has an accumulation of eosinophilic material in the acinar lumen (arrowed). (C) and (D) Sections of the gallbladder; the enlarged gallbladder of a $cftr^{G551D}/cftr^{G551D}$ animal (D), apparently healthy when sacrificed, shows a highly vacuolated epithelium [cf. wild-type sibling (C)] and evidence of an inflammatory infiltrate (arrowed). (E) and (F) Liver; the $cftr^{G551D}/cftr^{G551D}$ animal (F) shows a focal inflammatory infiltrate with an apparent absence of bile ducts when compared with a control sibling (E). (G) and (H) Submaxillary salivary gland; the serous cells of the $cftr^{G551D}/cftr^{G551D}$ animal (H) have lost some of their vacuolar appearance, as a result the gland appears hypercellular compared with a sibling control (G). For each tissue control and $cftr^{G551D}/cftr^{G551D}$ samples are shown at the same magnification. Scale bar: (A), (B), (E) and (F) 50 μm; (C) and (D) 20 μm; (G) and (H) 100 μm.

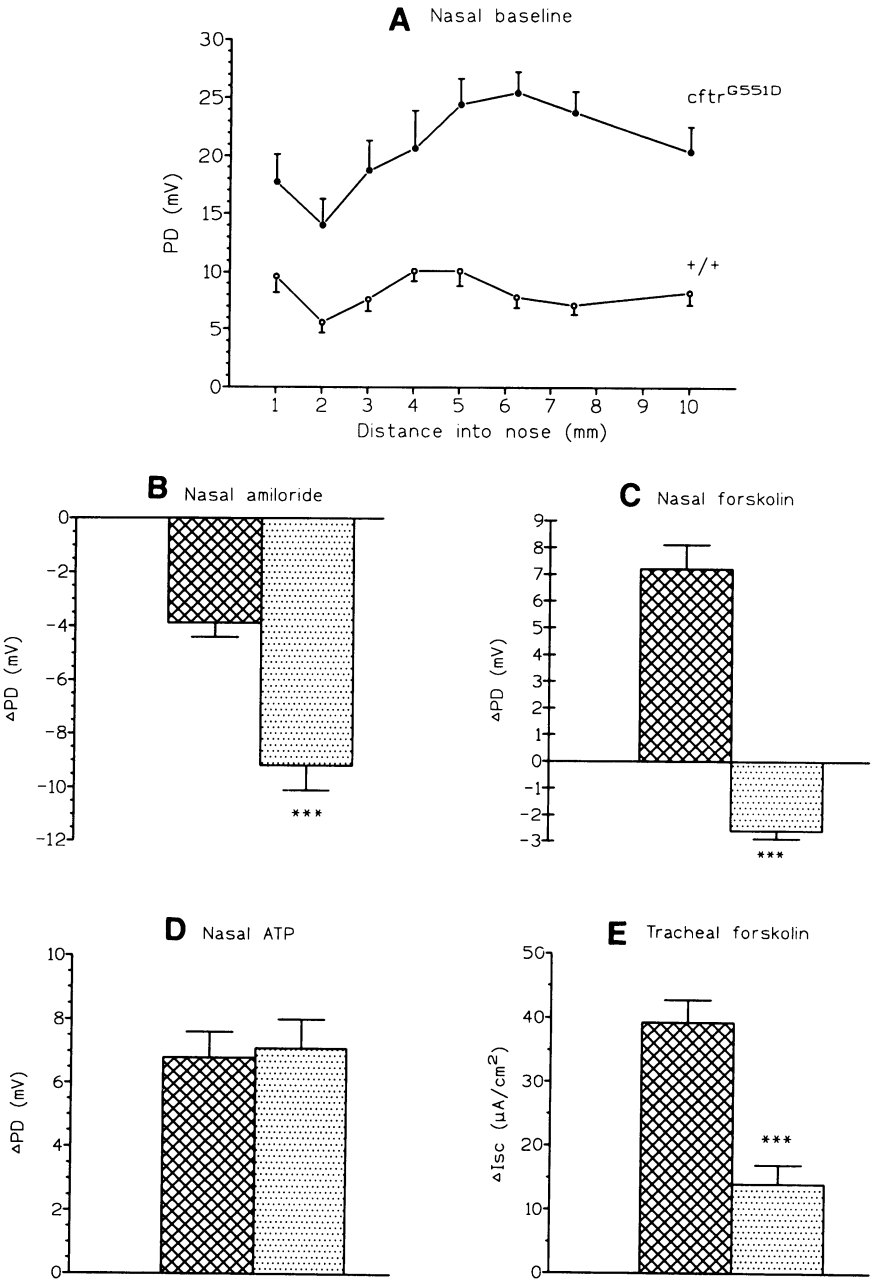

Fig. 5. Measurement of bioelectric responses in the airways of G551D mice. (A)–(D) *In vivo* recordings from the nasal epithelium; (E) *in vitro* recording from the tracheal epithelium. (**A**) Baseline nasal potential difference (PD) in $cftr^{G551D}/cftr^{G551D}$ mice (n = 7) in comparison with wild-type mice (n = 10). Comparison of maximal PD in $cftr^{G551D}/cftr^{G551D}$ versus +/+, $P<0.001$. (**B**) The response to perfusion with amiloride (100 μM). (**C**) The response to forskolin (10 μM) in a low Cl^- (6 mM) solution. (**D**) The response to perfusion with ATP (100 μM) in a low Cl^- (6 mM) solution. (**E**) The response to forskolin (10 μM) in $cftr^{G551D}/cftr^{G551D}$ mice (n = 7) and +/+ mice (n = 41). Baseline values were: $cftr^{G551D}/cftr^{G551D}$ 31.6 μA/cm^2 (5.3); +/+ 42.0 μA/cm^2 (3.8). Responses to amiloride were: $cftr^{G551D}$ −28.8 μA/cm^2 (8.6); +/+ −30.7 μA/cm^2 (3.0). Responses to ATP were: $cftr^{G551D}/cftr^{G551D}$ 111.4 μA/cm^2 (14.4); +/+ 70.4 μA/cm^2 (8.4), $P<0.05$. In each of the above, error bars indicate standard error of the mean (SEM). *** $P<0.01$. Hatched bars = +/+, speckled bars = $cftr^{G551D}/cftr^{G551D}$.

the increased longevity of these mice compared with $cftr^{m1UNC}$ 'null' mutants and reduced residual CFTR-related chloride transport function compared with $cftr^{m1HGU}$ mutants which have ~10% wild-type CFTR mRNA (Dorin *et al.*, 1994b). Further study is warranted to distinguish between a specific effect of the G551D mutation and a direct effect of limited CFTR function.

G551D CFTR is known to reach the apical membrane (Class III CFTR mutation), but probably demonstrates reduced residence time at this site (Prince *et al.*, 1994). Increases in cAMP levels inhibit the normal cycling of CFTR between the apical surface and an endocytic pool, but this inhibition does not occur with the G551D mutation. Furthermore, G551D demonstrates reduced nucleotide binding to the first nucleotide binding fold in which the mutation is localized (Logan *et al.*, 1994). Both these factors are likely to play a part in the markedly reduced function demonstrated here in the mutant mice and also reported in studies in cultured cells (Gregory *et al.*, 1991; Yang *et al.*, 1993) and *Xenopus* oocytes overexpressing

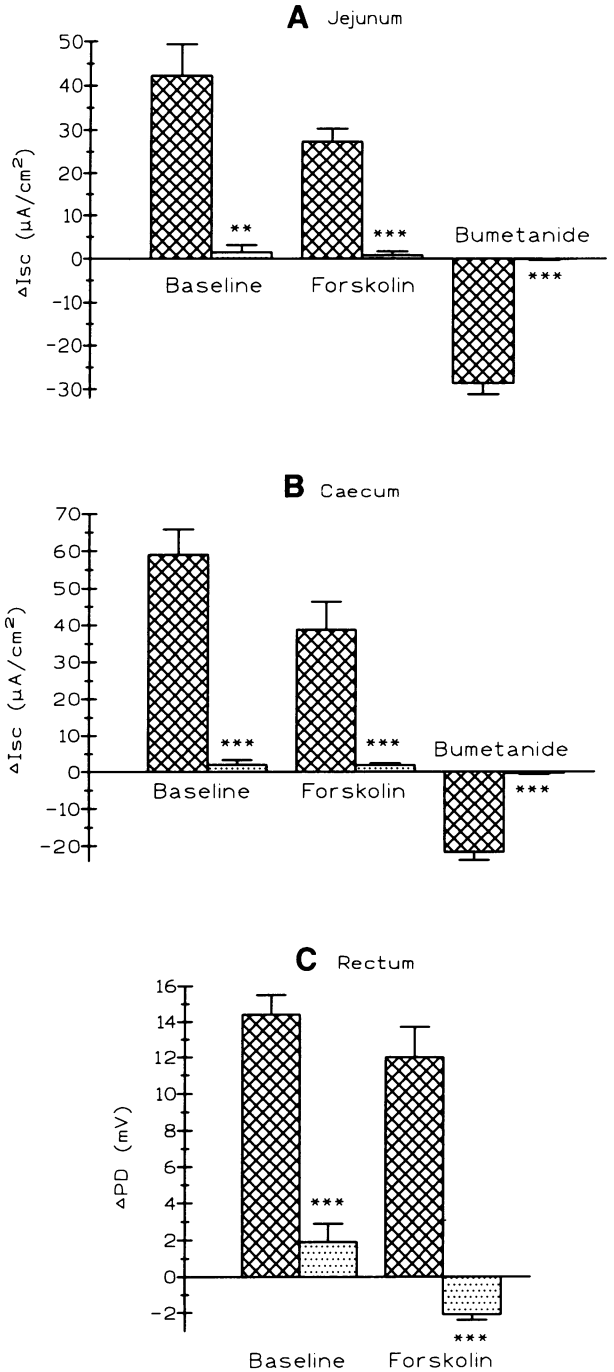

Fig. 6. Measurements of bioelectric responses in the intestine of $cftr^{G551D}/cftr^{G551D}$ animals. (**A**) Jejunum studied *in vitro*, +/+ n = 10; $cftr^{G551D}/cftr^{G551D}$ n = 7. (**B**) Caecum studied *in vitro*, +/+ n = 11; $cftr^{G551D}/cftr^{G551D}$ n = 7. (**C**) Rectum studied *in vivo* +/+ n = 9; $cftr^{G551D}/cftr^{G551D}$ n = 7. Conductance values were, jejunum: +/+ 14.6 mS/cm² (1.0), $cftr^{G551D}/cftr^{G551D}$ 19.0 mS/cm² (6.1); caecum: +/+ 16.9 mS/cm² (1.7), $cftr^{G551D}/cftr^{G551D}$ 14.0 mS/cm² (1.3); all conductance comparisons P = NS. In each figure, error bars indicate SEM. ***P<0.001. Hatched bars = +/+, speckled bars = $cftr^{G551D}/cftr^{G551D}$.

the mutant protein (Drumm *et al.*, 1991). In the latter *in vitro* studies, G551D demonstrated ~25–35% of the function produced by wild-type CFTR, in apparent marked contrast with our findings of an average value of 4% of wild-type responses in the mutant mice. The difference is most likely explained by the very different experimental systems studied and the inclusion of 3-isobutyl-1-methylxanthine (IBMX) in the stimulant cocktail. Phosphodiesterase inhibitors such as IBMX have been shown recently to activate G551D channels (Becq *et al.*, 1994), and suggest a therapeutic approach which may be tested in the $cftr^{G551D}$ mice.

Reduced cAMP, but not calcium-mediated chloride transport, was observed in the airways of the G551D mutants, as predicted from previous studies of CFTR function. We also demonstrate in the mouse that the G551D mutation increases sodium transport in the airways. To our knowledge, this has only been reported previously for CF subjects with either Class I 'null' mutations (and a complete absence of cellular CFTR) or Class II mutants, such as ΔF508 (in which the mutant protein is localized to the cytoplasm). Our results suggest that fully functional CFTR localized to the apical membrane appears to be necessary to prevent an increase in sodium absorption in the airways.

We measured a small, but significantly elevated response to forskolin in the caecum of G551D mice compared with 'null' mutants which had a marked effect on survival. As many as 67% of G551D mutant mice survived to 35 days when housed under specific pathogen-free conditions. Under conventional animal housing, survival was reduced to 27%, but this was still significantly higher than for complete 'null' mutants (8% survival; P<0.05). The improved survival of $cftr^{G551D}/cftr^{G551D}$ animals versus $cftr^{m1UNC}/cftr^{m1UNC}$ mice is in accord with the clinical picture where CF patients bearing the G551D allele are indistinguishable in all respects from ΔF508 homozygotes except for a 3-fold decrease in risk of meconium ileus (Hamosh *et al.*, 1992). This genotype–phenotype correlation is therefore substantiated across species, and the residual bioelectric responses in G551D animals probably explain these findings. The production of these G551D mice illustrates how mouse models carrying clinically relevant mutations may be of use in establishing mechanisms which underlie genotype–phenotype correlations.

The survival of the $cftr^{G551D}$ homozygous mice is clearly improved over that for the $cftr^{m1UNC}$ homozygotes, despite only a very low level of residual cAMP-mediated chloride conductance. This provides evidence for a phenotypic effect accruing from only a modest level of normal CFTR chloride channel function (in the caecum equivalent to ~5% of wild-type function). This is encouraging with respect to both gene therapy and pharmacological-based strategies for the treatment of CF. Our results also complement those of Zhou *et al.* (1994) who recently reported that transgenic expression of the human *CFTR* transgene driven by the FABP promoter, active in intestinal villus cells, restored ~30% of the cAMP-mediated chloride conductance, sufficient to substantially rescue the $cftr^{m1UNC}$ mutant strain from fatal intestinal disease.

The resulting good survival of the G551D mice means they provide an excellent model with which to study other aspects of CF pathogenesis, for example involving the lung and liver. We have recently shown that $cftr^{m1HGU}$ mice develop lung disease on exposure to CF-related pathogens (Davidson *et al.*, 1995). It will be of interest to establish whether the G551D mice, which have less residual CFTR function than the $cftr^{m1HGU}$ mice, develop more severe lung disease that might recapitulate the

chronic infection found in patients. These animals are the first CF mice to be produced to carry a Class III mutation, which occur in a significant number of CF patients. In contrast to the most common CFTR mutation (ΔF508), Class III mutations result in CFTR which is able to reach the apical membrane. These mice will therefore also be of value in testing treatment strategies that may only be applicable to this type of mutation, for example activation by pharmacological agents which alter CFTR regulation.

Materials and methods

Construction of the G551D targeting vector

A phage clone was isolated from an 129-Sv genomic library using a primer homologous to exon 11 sequences (nt 1721–1742) and contained exons 11, 11b, 12 and 13. The G551D mutation was introduced into exon 11 by PCR with Vent polymerase (New England Biolabs) using the primer (5′-CACTG AGTGG AGACC AGCGT GC-3′). Mutagenized clones were checked for PCR errors in coding regions, and a fragment containing exon 11 and 12 was used to replace the equivalent wild-type sequences in a subclone containing 6.3 kb of *Cftr* genomic DNA. A HSV-TK cassette was inserted at the 3′ end of the insert (Mansour *et al.*, 1988). Two *pgk–neo* cassettes (Tybulewicz *et al.*, 1991), as used in other *Cftr* replacement constructs (Koller *et al.*, 1991), were inserted 8 bp downstream of exon 11b.

Production of targeted lines and mutant mice

R1 ES cells were maintained and selected on primary embryonic fibroblasts (Wurst and Joyner, 1993) with leukaemia inhibitory factor (LIF) added to the media at 1000 U/ml. Chimaeric animals were produced by the aggregation method essentially as described for tetraploid aggregation by Nagy and Rossant (1993), except that a clump of 10–15 ES cells was placed in a well with a single CD-1 8 cell morula. Phenotype analysis of G551D mice was carried out on animals maintained in specific pathogen-free conditions on wood shaving bedding and standard rodent food (Norco Cooperative Ltd).

Allele-specific PCR

Amplification of DNA prepared from ES colonies or tail-tips for genotyping was carried out using the primers (5′-GACAT CACCA AGTTT GCAGA ACAAG-3′) and (5′-GTATA AAGCT TACCG GGTGT GGTG-3′) and a thermal profile of 95°C 30 s, 67°C 45 s, 72°C 1 min for 35 cycles. This primer pair produces a fragment of ~640 bp extending from the first nucleotide of exon 11 to 13 bp downstream of exon 11b and, in wild-type DNA, has a single *Bsa*I site 83 bp from the 3′ end. The mutagenesis of codon 551 results in the introduction of an additional *Bsa*I site such that PCR products from wild-type and $cftr^{G551D}$ alleles differ in length following digestion with *Bsa*I. Semi-quantitative RT-PCR of G551D transcripts was performed essentially as previously described (Delaney *et al.*, 1993). Products were quantitated by the inclusion of 1 μCi of [^{32}P]ATP in the PCR reaction. The primers used extend from exon 7 to exon 13 and were X7F2 (5′-GCCGT ACAGA TATGG TATGA TTC-3′) and SDCF 4 (5′-AAACT GGTCA AAAGT ATCAT ACC-3′). Reactions were terminated in the logarithmic phase of amplification. RT-PCR products corresponding to G551D transcripts can be distinguished from wild-type transcripts by the presence of a single *Bsa*I site.

Relative survival of the CFTR mutant mice

For the comparison of survival rates, animals were housed under conventional animal house conditions on Corn cob bedding (R.S.Biotech) and fed standard rodent food CRMX (Special Diet Services). $cftr^{m1UNC}$ mutant mice (Snouwaert *et al.*, 1992) were obtained from the Jackson Laboratories, Bar Harbor.

Histology

Dissected tissues were fixed in ice-cold 4% phosphate-buffered formaldehyde, embedded in paraffin wax and 6 μm sections were cut and stained with haematoxylin and eosin and periodic acid Schiffs (PAS) reagent. Liver and lung sections were examined with the genotype of the animal coded.

Electrophysiological methodology

Mice (weight 15–53 g) were anaesthetized (tribromoethanol 0.2 ml/10 g intraperitoneally) and a subcutaneous electrode inserted into a hind limb. Both this and the exploring electrode were connected by Krebs–HEPES of composition (mM): Na^+ 140, Cl^- 152, K^+ 6, Ca^{2+} 2, Mg^{2+} 1, glucose 10, HEPES 10 to a calomel electrode and, in turn, to a hand-held computer connected to a pre-amplifier containing a low-pass signal averaging filter with a time constant of 0.5 s. The offset of the electrodes was recorded prior to measurements, and appropriate corrections made. Buccal PD was used to validate the integrity of the circuit, acceptable values ranging from −10 to −17 mV. Rectal PD was measured using a double-lumen tube of outer diameter 1 mm, inserted to a distance of ~15 mm. Following the recording of stable values (± 0.2 mV over 15 s), drugs were perfused at a rate of 40 μl/min through the second lumen. Amiloride (100 μM) followed by forskolin (10 μM), each dissolved in Krebs–HEPES, were administered. Following these measurements, an opening was fashioned in the laryngeal cartilage and a tissue plug inserted. A tracheotomy was then made at the junction of the larynx and trachea. For nasal measurements, the exploring electrode consisted of a fine double-lumen plastic tube (outer diameter 0.5 mm) advanced into the left nasal cavity and the stable PD (± 0.5 mV over 15 s) recorded at ~1 mm intervals up to 10 mm. For drug perfusion, the exploring electrode was positioned 5 mm from the external nares. Drugs were perfused through the second lumen in the sequence: amiloride (100 μM in Krebs–HEPES), forskolin (10 μM) and ATP [100 μM, both in low chloride (6 mM) HEPES–Krebs with gluconate substitution]. The junctional potential between the normal bathing solution and the low-chloride solution was ignored because of paired comparisons. It is unlikely that the paracellular shunt is affected in CF airway epithelium (Widdicombe *et al.*, 1985).

Following *in vivo* measurements, animals were sacrificed, the trachea, and caecum dissected and placed in Krebs Henseleit solution of composition (mM): Na^+ 145.0, Cl^- 126.0, K^+ 5.9, Ca^{2+} 2.5, Mg^{2+} 1.2, HCO_3^- 26.0, PO_4^{2-} 1.2, SO_4^{2-} 1.2, glucose 5.6. The small intestine was placed in an equivalent solution, with the glucose replaced by equimolar mannitol. All tissues were transported to the laboratory on ice and mounted in Ussing chambers of aperture diameter 0.28 cm^2 (jejunum and caecum) or 0.03 cm^2 (trachea). Two chambers were obtained from each jejunum and caecum and one from the trachea. Values were subsequently meaned to provide a single measurement for each animal. Both mucosal and serosal surfaces of the tissues were bathed in Krebs Henseleit solution at 37°C, pH 7.4, circulated by 95% O_2/5% CO_2, with the exception of the jejunum, where glucose was replaced with equimolar mannitol on the mucosal surface. Studies were performed under short-circuit conditions. Prior to and at the peak/trough of each drug intervention, a 2 μA pulse was passed to allow measurement of tissue conductance. In the trachea, once stable values were attained, tissues were treated sequentially with amiloride (100 μM), forskolin (10 μM) and ATP (100 μM). All drugs were added mucosally. In the jejunum, the sequence of additions was forskolin (10 μM, serosally), ionomycin (5 μM, bilaterally), bumetanide (100 μM, serosally), glucose (5.5 mM, mucosally) and phloridzin (200 μM, mucosally). In the caecum, the sequence of additions was forskolin (10 μM, serosally), ionomycin (5 μM, bilaterally) and bumetanide (100 μM, serosally). Recordings from all animals studied are included in the analyses, with the exception of one animal ($cftr^{m1UNC}/cftr^{m1UNC}$) in which no measurements could be obtained because of technical difficulties. All statistical comparisons were made using the Mann–Whitney U test; the null hypothesis was rejected at $P<0.05$.

Acknowledgements

We are grateful to Julie Conway, Laurel Kelly and the Biosciences Unit of the National Heart and Lung Institute for animal husbandry, and to Sheila Webb, Fiona Gulliver and Paul Addison for technical assistance. We are indebted to Andras Nagy for the gift of R1 cells and thank Duncan Geddes for helpful discussions. S.J.D. acknowledges a Wellcome Ramaciotti Foundation Travel Award. J.R.D. is a Caledonian Research Fellow and E.W.F.W.A. is a Wellcome Trust Senior Clinical Fellow. This study was funded by the National Health and Medical Research Council of Australia, the Medical Research Council UK, the Cystic Fibrosis Trust UK, the Association Française contre la Lutte Mucoviscidose (Artemis program), the Australian Cystic Fibrosis Association and the Cystic Fibrosis Association of Queensland.

References

Alton,E.W.F.W. *et al.* (1993) *Nature Genet.*, **5**, 135–142.

Becq,F., Jensen,T. J., Chang,X.-B., Savoia,A., Rommens,J.M., Tsui,L.-C., Buchwald,M., Riordan,J.R. and Hanrahan,J.W. (1994) *Proc. Natl Acad. Sci. USA*, **91**, 9160–9164.

Davidson,D.J., Dorin,J.R., McLachlan,G., Ranaldi,V., Lamb,D., Doherty,C., Govan,J. and Porteous,D.J. (1995) *Nature Genet.*, **9**, 351–357.

Delaney,S.J., Rich,D.P., Thomsom,S.A., Hargrave,M.R., Lovelock,P.K., Welsh,M.J. and Wainwright,B.J. (1993) *Nature Genet.*, **4**, 426–430.

Dorin,J.R. *et al.* (1992) *Nature*, **359**, 211–215.

Dorin,J.R., Alton,E.W.F.W. and Porteous,D.J. (1994a) In Dodge,J.A., Brock,D.J.H. and Widdicombe,J.H. (eds), *Cystic Fibrosis—Current Topics*. John Wiley and Sons, Chichester, UK, Vol. 2, pp. 3–33.

Dorin,J.R., Stevenson,B.J., Fleming,S., Alton,E.W.F.W., Dickinson,P. and Porteous,D.J. (1994b) *Mammalian Genome*, **5**, 465–472.

Drumm,M.L., Wilkinson,D.J., Smit,L.S., Worrell,R.T., Strong,T.V., Frizzell,R.A., Dawson,D.C. and Collins,F.S. (1991) *Science*, **254**, 1797–1799.

Gregory,R.J., Rich,D.P., Cheng,S.H., Souza,D.W., Paul,S., Manavalan,P., Anderson,M.P., Welsh,M.J. and Smith,A.E. (1991) *Mol. Cell. Biol.*, **11**, 3886–3893.

Grubb,B.R., Pickles,R.J., Ye,H., Yankaskas,J.R., Vick,R.N., Engelhardt, J.F., Wilson,J.M., Johnson,L.G. and Boucher,R.C. (1994) *Nature*, **371**, 802–806.

Hamosh,A. and Cutting,G. (1993) In Dodge,J.A., Brock,D.J.H. and Widdicombe,J.H. (eds), *Cystic Fibrosis—Current Topics*. John Wiley and Sons, Chichester, UK, Vol.1, pp. 69–92.

Hamosh,A. *et al.* (1992) *Am. J. Hum. Genet.*, **51**, 245–250.

Hyde,S.C., Gill,D.R., Higgins,C.F., Trezise,A.E.O., Mac Vinish,L.J., Cuthbert,A.W., Ratcliff,R., Evans,M.J. and Colledge,W.H. (1993) *Nature*, **362**, 250–255.

Koller,B.H., Kim,H.S., Latour,A.M., Brigman,K., Boucher,R.J., Scambler,P., Wainwright,B. and Smithies,O. (1991) *Proc. Natl Acad. Sci. USA*, **88**, 10730–10734.

Logan,J., Hiestand,D., Daram,P., Huang,Z., Muccio,D.D., Hartman,J., Haley,B., Cook,W.J. and Sorscher,E.J. (1994) *J. Clin. Invest.*, **94**, 228–236.

Mansour,S.L., Thomas,K.R. and Capecchi,M.C. (1988) *Nature*, **336**, 348–352.

Nagy,A. and Rossant,J. (1993) In Joyner,A.L. (ed.), *Gene Targeting—A Practical Approach*. Oxford University Press, Oxford, UK, pp. 147–179.

Park,R.W. and Grand,R.J. (1991) *Gastroenterology*, **81**, 1143–1161.

Prince,L.S., Workman,R.J. and Marchase,R.B. (1994) *Proc. Natl Acad. Sci. USA*, **91**, 5192–5196.

Ratcliff,R., Evans,M.J., Cuthbert,A.W., MacVinish,L.J., Foster,D., Anderson,J.R. and Colledge,W.H. (1993) *Nature Genet.*, **4**, 35–41.

Snouwaert,J.N., Brigman,K.K., Latour,A.M., Malouf,N.N., Boucher, R.C., Smithies,O. and Koller,B.H. (1992) *Science*, **257**, 1083–1088.

Tsui,L.-C. (1992) *Trends Genet.*, **8**, 392–398.

Tybulewicz,V.L.J., Crawford,C.E., Jackson,P.K., Bronson,R.T. and Mulligan,R.C. (1991) *Cell*, **65**, 1153–1163.

Welsh,M.J. and Smith,A.E. (1993) *Cell*, **73**, 1251–1254.

Widdicombe,J.H., Welsh,M.J. and Finkbeiner,W.E. (1985) *Proc. Natl Acad. Sci. USA*, **82**, 6167–6171.

Wurst,W. and Joyner,A.L. (1993) In Joyner,A.L. (ed.), *Gene Targeting—A Practical Approach*. Oxford University Press, Oxford, UK, pp. 33–61.

Yang,Y., Devor,D.C., Engelhardt,J.F., Ernst,S.A., Strong,T.V., Collins, F.S., Frizzell,R.A. and Wilson,J.M. (1993) *Hum. Mol. Genet.*, **2**, 1253–1261.

Zhou,L., Dey,C.R., Wert,S.E., DuVall,M.D., Frizzell,R.A. and Whitsett,J.A. (1994) *Science*, **266**, 1705–1708.

Received on July 31, 1995; revised on October 9, 1995